NLO QCD corrections to pp → t̄tb̄b̄

A. Bredenstein

High Energy Accelerator Research Organization (KEK), Tsukuba, Ibaraki 305-0801, Japan

A. Denner

Paul Scherrer Institut, Würenlingen und Villigen, CH-5232 Villigen PSI, Switzerland
E-mail: ansgar.denner@psi.ch

S. Dittmaier[∗]

Albert-Ludwigs-Universität Freiburg, Physikalisches Institut, D-79104 Freiburg, Germany
E-mail: stefan.dittmaier@physik.uni-freiburg.de

S. Pozzorini

Physics Department, Theory Group, CERN, CH-1211 Geneva 23, Switzerland
E-mail: stefano.pozzorini@cern.ch

We summarise predictions for t̄tb̄b production at the LHC in next-to-leading order QCD. The precise description of this background process is a prerequisite to observe associated t̄tH production in the H → b̄b decay channel. The one-loop amplitudes are computed using Feynman diagrams and numerical tensor reduction. This approach provides very high numerical stability and CPU efficiency. We find that the scale choice adopted in ATLAS simulations underestimates the t̄tb̄b background by a factor two and introduce a new dynamical scale that stabilises the perturbative predictions. In the regime of highly boosted Higgs bosons, which offers better perspectives to observe the t̄tH(H → b̄b) signal, the corrections induce significant distortions in the kinematic distributions.

[∗]Speaker.

1. Introduction

The discovery of the Higgs boson and the measurement of its couplings represent a central goal of the Large Hadron Collider (LHC). For a light Higgs boson, $M_H \lesssim 130\,$GeV, associated tt̄H(H → bb̄) production provides the opportunity to measure the top-quark Yukawa coupling. However, the extraction of this signal from its large QCD backgrounds, pp → tt̄bb̄ and tt̄jj, represents a serious challenge. The selection strategies elaborated by ATLAS and CMS [1, 2] anticipate a statistical significance around 2σ and a signal-to-background ratio as low as 1/10. This calls for better than 10% precision in the background description, a very demanding requirement both from the experimental and theoretical point of view. Recently, a novel selection strategy based on highly boosted Higgs bosons has opened new and very promising perspectives [3], suggesting an increase in the signal-to-background ratio beyond 1/3.

The calculation of the next-to-leading-order (NLO) QCD corrections to the irreducible tt̄bb̄ background, first presented in Refs. [4, 5, 6] and subsequently confirmed in Ref. [7], constitutes another important step towards the observability of tt̄H(H → bb̄) at the LHC. These NLO predictions are mandatory in order to reduce the huge scale uncertainty of the lowest-order (LO) tt̄bb̄ cross section, which can vary up to a factor four if the QCD scales are identified with different kinematic parameters [8]. In the following we give a brief account of our calculation of NLO QCD corrections to pp → tt̄bb̄ and refer to the original papers [4, 5, 6] for more details and results.

The calculation of the NLO corrections to pp → tt̄bb̄ constitutes also an important technical benchmark. The description of many-particle processes at NLO plays a central role for the LHC physics programme, and the technical challenges raised by these calculations have triggered an impressive amount of conceptual and technical developments. Within the last year, this progress has lead to the first NLO results for six-particle processes at the LHC, namely for pp → tt̄bb̄ [5, 7], pp → tt̄jj [9], for the leading- [10] and the full-colour contributions [11] to pp → Wjjj, for pp → Z/γjjj [12], for the $q\bar{q}$ contribution to pp → bb̄bb̄ [13], and for the QCD-induced production of W⁺W⁺jj final states [14].

2. Outline of the calculation

In LO, the hadronic production of tt̄bb̄ proceeds via the partonic processes $q\bar{q}$ → tt̄bb̄ and gg → tt̄bb̄, which are described by 7 and 36 tree diagrams, respectively. The corresponding virtual NLO QCD corrections involve 188 and 1003 one-loop diagrams. The real emission contributions comprise the crossing-symmetric channels $q\bar{q}$ → tt̄bb̄g, qg → tt̄bb̄q, and g$\bar{q}$ → tt̄bb̄$\bar{q}$, which involve 64 tree diagrams each, and the channel gg → tt̄bb̄g with 341 diagrams. Each of these contributions has been worked out twice and independently, resulting in two completely independent computer codes.

The virtual corrections are calculated in the Feynman-diagrammatic approach. The diagrams are generated with two independent versions of FEYNARTS [16] and algebraically simplified with two in-house MATHEMATICA programs that generate FORTRAN77 code in a fully automatised way. One of the two programs relies on FORMCALC 5.2 [17] for preliminary algebraic manipulations. The virtual corrections are obtained from the interference of the one-loop and LO matrix elements on a diagram-by-diagram basis.

Owing to colour factorisation for individual (sub)diagrams colour sums can be performed very efficiently. The colour-summed result is given by a combination of previously computed colour–Born interference terms. This requires *a single evaluation* of the non-trivial colour-stripped amplitude of each (sub)diagram. Helicity structures are handled in a similar way. The helicity-dependent parts of all diagrams are reduced to a common basis of so-called Standard Matrix Elements (SMEs), and helicity sums are performed once and for all at the level of the SMEs–Born interference. The diagram-independent treatment of the helicity-dependent parts of loop graphs is made possible by the covariant decomposition of tensor integrals.

The one-loop amplitudes are expressed as linear combinations of tensor-integral coefficients. The latter are evaluated by two independent *numerical* FORTRAN libraries that recursively reduce them to master integrals using the methods of Ref. [15]. Avoiding an explicit reduction of analytic expressions to master integrals, this numerical approach prevents prohibitively large expressions and permits to adapt the reduction strategy to the specific numerical problems that appear in different phase-space regions. An automatic cache system is implemented that strongly boosts the reduction by recycling a multitude of tensor integrals among Feynman diagrams with common sub-topologies.

Ultraviolet (UV) divergences are regularized dimensionally throughout, but infrared (IR) divergences are treated in different variants, which comprise pure dimensional regularization with strictly massless light quarks and a hybrid scheme with small quark masses. The corresponding scalar integrals are evaluated using the methods and results of Ref. [18, 19], and different regularization schemes are translated into each other as described in Ref. [20]. The treatment of rational parts is greatly simplified by the fact that rational terms resulting from $1/\varepsilon$ and $1/\varepsilon^2$ poles of IR kind vanish in truncated one-loop amplitudes [4]. Rational terms arising from UV poles of tensor integrals with D-dependent coefficients are automatically extracted by means of a catalogue of residues.

To handle singularities in the real corrections we employed the dipole subtraction method [21], in particular the MADDIPOLE implementation [22] in one of our calculations. The $2 \to 5$ matrix elements were generated with MADGRAPH [23] and checked against analytic calculations with the Weyl–van der Waerden spinor formalism and in-house code based on off-shell recursions.

3. Predictions for the LHC

We study the process pp → t̄t̄bb̄ + X at $\sqrt{s} = 14\,\text{TeV}$ with $m_\text{t} = 172.6\,\text{GeV}$ and massless b quarks. Massless final-state partons with rapidity–azimuthal-angle separation $\sqrt{\Delta\phi^2 + \Delta y^2} < D = 0.4$ are recombined into jets using a k_T-algorithm, and we require two b jets with $p_{\text{T,b}} > 20\,\text{GeV}$ and $|y_\text{b}| < 2.5$. We use the CTEQ6 set of PDFs but neglect the suppressed contributions from b quarks in the initial state. More details are given in Ref. [6].

In all recent ATLAS studies of t̄tH(H → bb̄) [1, 8, 24] the signal and its t̄t̄bb̄ background were simulated by setting the renormalisation and factorisation scales equal to half the threshold energy, $E_\text{thr} = 2m_\text{t} + m_{\text{b}\bar{\text{b}}}$. In Ref. [5] we found that for this scale choice the NLO corrections to pp → t̄t̄bb̄ are close to a factor of two. This enhancement is due to the fact that pp → t̄t̄bb̄ is a multi-scale process involving various scales well below $E_\text{thr}/2$. The inspection of differential distributions reveals that the cross section is saturated by b quarks with $p_{\text{T,b}} \ll m_\text{t}$. Therefore we introduced in
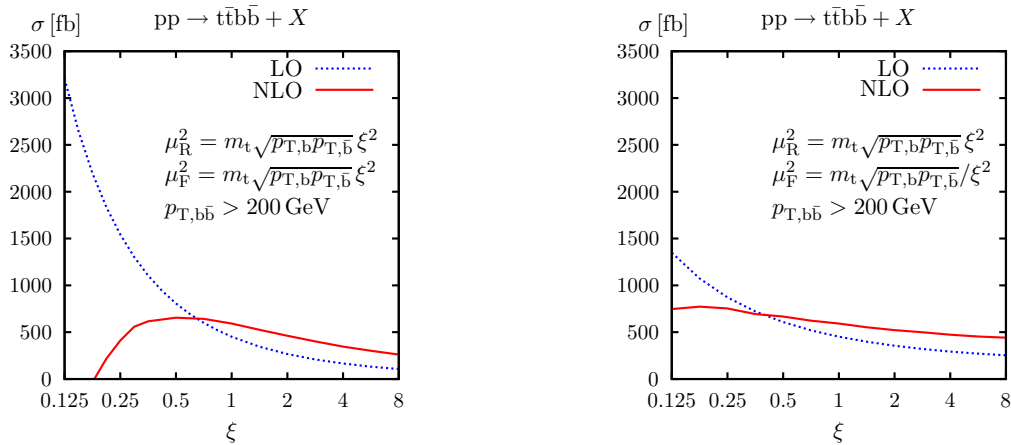
3

Figure 1: Scale dependence of the LO and NLO pp → tt̄bb̄ + X cross section. The left and the right plots describe uniform ($\xi_R = \xi_F = \xi$) and antipodal ($\xi_R = \xi_F^{-1} = \xi$) scale variations, respectively.
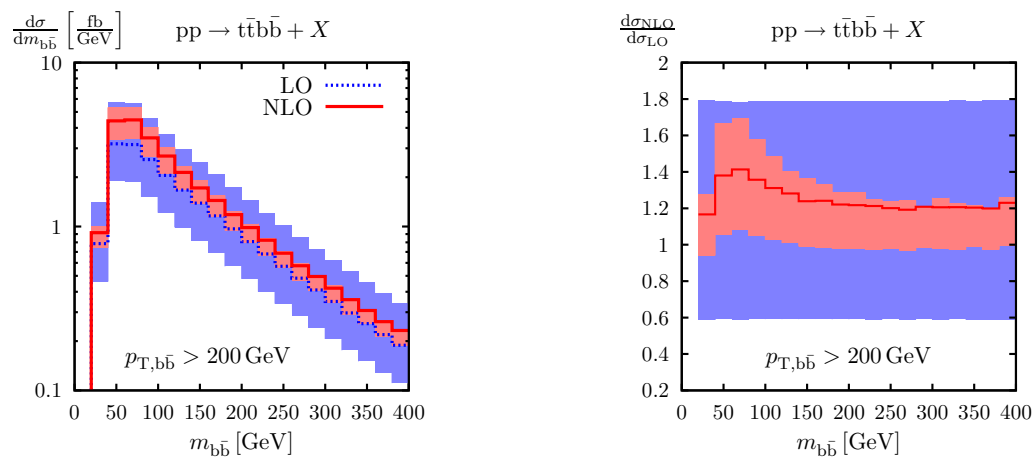

Figure 2: Invariant-mass distribution of the bb̄ pair: absolute LO and NLO predictions (left) and NLO K factor (right).

Ref. [6] the dynamical scale $\mu_0^2 = m_t \sqrt{p_{T,b} p_{T,\bar{b}}}$, which improves the perturbative convergence and minimises NLO effects in the shape of distributions.

Using this dynamical scale, we discussed in Ref. [6] the kinematic region $m_{b\bar{b}} > 100 \, \text{GeV}$ and found that for all distributions considered the NLO corrections are at the level of 20–30% and have relatively little impact on the shape of distributions. On the other hand, the corrections still induce significant distortions of the kinematic distributions in the regime of a highly boosted Higgs boson. Here we provide some results for this scenario with $p_{T,b\bar{b}} > 200 \, \text{GeV}$.

In Figure 1 we show the scale dependence of the LO and NLO integrated cross sections. Renormalisation (μ_R) and factorisation (μ_F) scales are varied around the central value, $\mu_R = \xi_R \mu_0$, $\mu_F = \xi_F \mu_0$ in a uniform ($\xi_F = \xi_R$) and antipodal ($\xi_F = \xi_R^{-1}$) way in the range $1/8 \leq \xi_F, \xi_R \leq 8$. At the central scale we obtain $\sigma_{LO} = 451.8(2) \, \text{fb}$ and $\sigma_{NLO} = 592(4) \, \text{fb}$ corresponding to $K = 1.31$. The shape of the scale-dependence curves indicates good convergence and stability of the perturbative expansion. The shifts induced by factor-two variations of the QCD scales amount to 79% in LO and 22% in NLO.

4

The bb̄ invariant-mass distribution is displayed in Figure 2 where the LO and NLO uncertainty bands result form factor-two uniform scale variations, which have a larger impact as antipodal variations. More precisely, the distributions are evaluated at three different scales: $\xi_F = \xi_R = 0.5, 1, 2$. The NLO corrections induce an appreciable shape distortion of about 20%, in particular near the physically interesting region of $m_{b\bar{b}} \sim 100\,\mathrm{GeV}$. Such an effect tends to mimic a Higgs signal and should be carefully taken into account in the tt̄H(H → bb̄) analysis. For other distributions the shape distortion is not as sizeable.

References

[1] G. Aad *et al.* [The ATLAS Collaboration], arXiv:0901.0512 [hep-ex].

[2] G. L. Bayatian *et al.* [CMS Collaboration], J. Phys. G **34** (2007) 995.

[3] T. Plehn, G. P. Salam and M. Spannowsky, Phys. Rev. Lett. **104**, 111801 (2010).

[4] A. Bredenstein, A. Denner, S. Dittmaier and S. Pozzorini, JHEP **0808** (2008) 108.

[5] A. Bredenstein, A. Denner, S. Dittmaier and S. Pozzorini, Phys. Rev. Lett. **103** (2009) 012002.

[6] A. Bredenstein, A. Denner, S. Dittmaier and S. Pozzorini, JHEP **1003** (2010) 021.

[7] G. Bevilacqua *et al.*, JHEP **0909** (2009) 109.

[8] B. P. Kersevan and E. Richter-Was, Eur. Phys. J. C **25** (2002) 379; Comput. Phys. Commun. **149**, 142 (2003).

[9] G. Bevilacqua, M. Czakon, C. G. Papadopoulos and M. Worek, Phys. Rev. Lett. **104**, 162002 (2010).

[10] R. Keith Ellis, K. Melnikov and G. Zanderighi, Phys. Rev. D **80**, 094002 (2009).

[11] C. F. Berger *et al.*, Phys. Rev. D **80** (2009) 074036.

[12] C. F. Berger *et al.*, arXiv:1004.1659 [hep-ph].

[13] T. Binoth, *et al.*, Phys. Lett. B **685** (2010) 293.

[14] T. Melia, K. Melnikov, R. Rontsch and G. Zanderighi, arXiv:1007.5313 [hep-ph].

[15] A. Denner and S. Dittmaier, Nucl. Phys. B **658** (2003) 175; Nucl. Phys. B **734** (2006) 62.

[16] J. Küblbeck, M. Böhm and A. Denner, Comput. Phys. Commun. **60** (1990) 165; H. Eck and J. Küblbeck, *Guide to FeynArts 1.0*, University of Würzburg, 1992; T. Hahn, Comput. Phys. Commun. **140** (2001) 418.

[17] T. Hahn and M. Pérez-Victoria, Comput. Phys. Commun. **118** (1999) 153; T. Hahn, Nucl. Phys. Proc. Suppl. **89** (2000) 231.

[18] G. 't Hooft and M. Veltman, Nucl. Phys. B **153** (1979) 365; W. Beenakker and A. Denner, Nucl. Phys. B **338** (1990) 349; A. Denner, U. Nierste and R. Scharf, Nucl. Phys. B **367** (1991) 637.

[19] A. Denner and S. Dittmaier, arXiv:1005.2076 [hep-ph].

[20] S. Dittmaier, Nucl. Phys. B **675** (2003) 447.

[21] S. Catani, S. Dittmaier, M. H. Seymour and Z. Trócsányi, Nucl. Phys. B **627** (2002) 189.

[22] R. Frederix, T. Gehrmann and N. Greiner, JHEP **0809** (2008) 122.

[23] J. Alwall *et al.*, JHEP **0709** (2007) 028.

[24] J. Cammin and M. Schumacher, ATL-PHYS-2003-024.